

Characterization of Copper Coatings Deposited by High-Velocity Oxy-Fuel Spray for Thermal and Electrical Conductivity Applications

H.R. SALIMIJAZI,^{1,3} M. AGHAEI,¹ M. SALEHI,¹ and E. GARCIA²

1.—Department of Materials Engineering, Isfahan University of Technology, Isfahan 84156-83111, Iran. 2.—Institute of Ceramics and Glass, ICV-CSIC, Kelsen, 28049 Madrid, Spain. 3.—e-mail: hrjazi@cc.iut.ac.ir

Copper coatings were deposited on steel substrates by high-velocity oxy-fuel spraying. The microstructure of the feedstock copper powders and free-standing coatings were evaluated by optical and scanning electron microscopy. The x-ray diffraction pattern was utilized to determine phase compositions of powders and coatings. Oxygen content was determined by a LECO-T300 oxygen determiner. The thermal conductivity of the coatings was measured in two directions, through-thickness and in-plane by laser flash apparatus. The electrical resistivity of the coatings was measured by the four-point probe method. Oxygen content of the coatings was two times higher than that of the initial powders (0.35–0.37%). The thermal and electrical conductivities of the coatings were different depending on the direction of the measurement. The thermal and electrical conductivity of the coatings improved after annealing for 6 h at a temperature of 600°C.

INTRODUCTION

Copper coatings are widely used in industry including coating the surface of printing and casting rolls in steel galvanizing plants due to their high thermal and electrical conductivity. Thermal spray processes can make a dense coating with acceptable porosity and oxide content which exhibit good performance.

The limited flame temperature and high velocity of particles (~ 1000 m/s) in high-velocity oxy-fuel spraying (HVOF) prevent excessive metal oxidation and porosity ($< 2\%$). An important feature of such coatings is the anisotropy of physical properties such as thermal and electrical conductivity. The anisotropy of the electrical resistivity or thermal conductivity is defined as the ratio of the through-thickness resistivity (ρ_{tt}) or conductivity (λ_{tt}) to in-plane resistivity (ρ_{ip}) or conductivity (λ_{ip}). This anisotropy may arise from the anisotropic shape, size, and distribution of defects as well as the lamellae structure of the coatings. The splat–splat interfaces could play an important role in reducing

conductivity in the through-thickness direction due to the formation of transition regions produced by rapid cooling.^{1–3}

Microstructural evaluation showed that the individual splats morphology and interfaces play important roles in thermal and electrical conductivity.⁴ Other studies surveyed the mechanical properties of copper coatings.^{4–6} They concluded that the high hardness (about 90% of cold-rolled copper sheet) obtained for cold spray and HVOF-sprayed coatings is due to solid-state deformation during deposition. Liu et al.⁷ studied the microstructure and properties of Cu coating on a diamond-Cu substrate by the HVOF process. Their coating was dense ($< 1\%$ porosity) with $< 0.5\%$ oxygen content, and thermal conductivity was about 266 W/m K. The microstructure of the Cu coatings and their electrical resistivity and microhardness could be modified through a post-spraying annealing treatment. Post-deposition annealing could lead to an evident recrystallization of the deformed grains and remarkable grain growth which improves the interface bonding between deposited particles.^{8,9}

The microstructure of the Cu coating such as porosity and oxide content depends on the HVOF process parameters such as the ratio of oxygen to kerosene. The purpose of this paper is to study the microstructure evolution of Cu coatings deposited by different ratios of oxygen to kerosene. Moreover, the relationship between the microstructure characteristics and the anisotropy of the electrical resistivity and the thermal conductivity of the coatings will be investigated before and after the annealing treatment. These relationships will be derived in the explicit quantitative form, in terms of the appropriate microstructural parameters. Such parameters reflect the average splat length and also the number of splat-splat interfaces in the microstructure.

EXPERIMENTAL PROCEDURE

Coatings were prepared by HVOF thermal spraying (Metallisation-Metjet III; Metallisation, West Midlands, UK). The initial copper powder particles, supplied by GTV, Luckenbach, Germany ($45 \pm 10 \mu\text{m}$), were sieved from $25 \mu\text{m}$ to $45 \mu\text{m}$ by a particle sizer (analysette 22; Fritsch, Germany). The coatings were deposited on low-carbon steel plates based on the recommended process parameters by the HVOF manufacturer. Three different ratios of kerosene to oxygen were chosen to study the effect of process parameters on the oxide content of the coatings (Table SI, Supplemental). After deposition, coatings were removed from the substrates. All the parameters except the oxygen and kerosene flow rates were kept constant in all conditions. Oxide content of coatings was measured using an oxygen determiner (LECO-T300). The phase structure of the sieved powders and coatings were characterized by x-ray diffraction measurement (Philips, X'pert). Microstructural inspections were performed by scanning electron microscopy on the sieved powder particles and coatings to characterize the coating morphology and splat boundaries. The as-polished cross-sections of the Cu coatings were etched using a solution of 5 g $\text{FeCl}_3 + 10 \text{ mL HCl} + 100 \text{ mL H}_2\text{O}$ for microstructure examination. The coating porosity and splat interface area were measured by digital image analysis of the polished cross-section of the optical micro-images using Clemex software package v.3.5 from Clemex Technologies. The average length of splats was measured by image analysis from the polished cross-section of the coatings using Image Tool software v.3 from the Department of Dental Diagnostic Science at The University of Texas Health Science Center, San Antonio, TX, USA.

Hardness measurements were performed on the polished cross-sections using a Vickers indenter at a load of 300 g (HV0.3, DIN 50133). Post-deposition heat treatment of the as-sprayed specimens was carried out at 600°C for 6 h under controlled argon atmosphere condition.

The through-thickness thermal diffusivity in the direction parallel to the thermal spray axis ($\alpha_{\text{through-thickness}}$) was measured in Ar atmosphere at room temperature on $8.8 \times 8.8 \text{ mm}^2$ specimens with around 1 mm thickness by the laser-flash method (Thermaflash 2200; Holometrix Netzsch, USA). Data are averaged over at least three measurements. In-plane measurements of the radial thermal diffusivity ($\alpha_{\text{In-plane}}$) at room temperature were carried out using a special arrangement that fits into the laser-flash equipment. The specific heat at room temperature (C_p) was taken from Tables (0.385 J/g K). The densities of the free-standing coatings were measured by Archimedes method. The thermal conductivity (k) was then calculated from the thermal diffusivity, the density, and the tabulated specific heat, using the following expression:

$$k = \alpha \rho C_p \quad (1)$$

The estimated accuracy of the laser-flash technique is 7% for the through-thickness and in-plane thermal conductivity measurements.

The electrical resistivity measurements were performed in two directions for the free-standing coatings with a thickness ranging from 1 mm to 3 mm. The four-contact method was employed for measurement. The process of preparation of samples is shown schematically in supplemental Fig. S1.

RESULTS AND DISCUSSION

Copper Powders

Since the oxygen content of coatings depends on the initial powder particle size,¹⁰ the initial powders were sieved to obtain a larger particle size. Size distributions of powders before and after sieving are shown in supplemental Fig. S2. In the sieved state, over 80% of powder particles are larger than $25 \mu\text{m}$. Figure S3a (supplemental) shows the SEM morphology of the sieved copper powder particles used for HVOF spraying, and Fig. S3b (supplemental) shows an optical image from the cross-sectional microstructure of powders consist of copper grains with an average grain size of $5 \mu\text{m}$. The powder particles have irregular shapes and the powder particles smaller than $20 \mu\text{m}$ sizes were eliminated during the sieving process. The oxygen content of the powder was about $0.152 \pm 0.020 \text{ wt.}\%$.

Coatings Microstructure

Figure 1 shows the as-sprayed and annealed microstructure of coatings deposited by using the HVOF process parameters described in Table I (supplemental). HVOF-sprayed copper coatings showed a quite non-uniform microstructure with some oxidized lamellar regions in the splat boundaries. By image analysis of the etched cross-

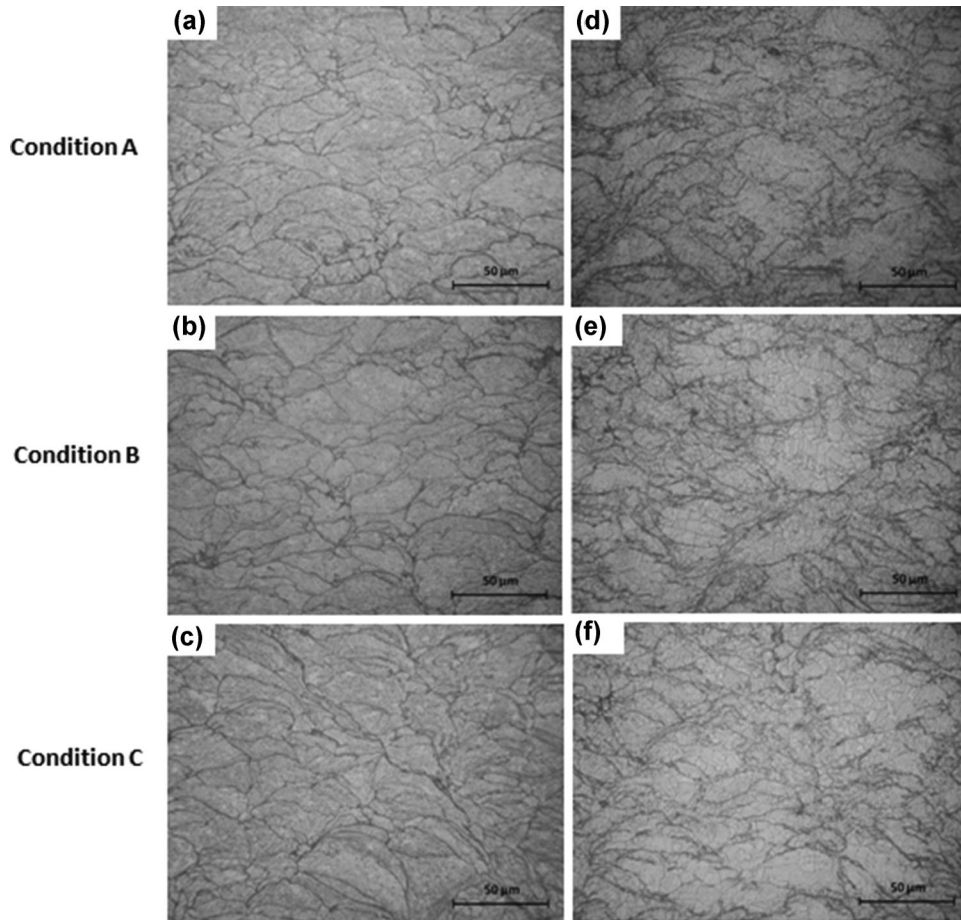


Fig. 1. Microstructure of HVOF-sprayed copper coatings in (a–c) as-sprayed conditions, and (d–f) after heat treatment.

sections, the amount of splat boundaries was estimated to be in the range of 8–16% where the lower level is attributed to the annealed samples. Because of diffusion of copper atoms across the splat boundaries, the number of splat interfaces decreased after heat treatment. The measurement of the splat dimensions in two directions reveals that the average size of splats increased after annealing. This shows that some splat interfaces merged during annealing and the average number of splat interfaces decreased. The porosity percentage of all measured coatings was $< 1.5\%$.

The x-ray diffraction patterns of the powders, as-sprayed, and annealed specimens indicated that there are no significant differences in the feedstock powder and as-sprayed patterns (Fig. 4 in supplemental). However, slight broadening of the peaks could be detected in the as-sprayed specimen. This could be attributed to the rapid solidification and high level of residual stresses in the microstructure. The peaks broadening was reduced after annealing. This could be attributed to the reduction of the residual stresses and grain growth in the microstructure.

Coatings Microhardness

Microhardness of the as-sprayed coatings was in the range of $130 \pm 5 \text{ HV}_{0.3}$ which decreased after annealing to $85 \pm 5 \text{ HV}_{0.3}$. Higher hardness of the as-sprayed coatings refers to finer grain size and higher dislocation density due to rapid solidification during high-velocity impact of molten particles onto the substrate. Investigations of cold-sprayed copper coatings have shown that high dislocation density and strain hardening in these types of coatings are responsible for obtaining a high value of microhardness ($150 \text{ HV}_{0.3}$).^{11,12} Moreover, oxygen content of the initial powder and deposited coatings could have strong influences on the adhesion strength and microstructure of the cold-sprayed coatings.^{13,14} During annealing, the recovery and recrystallization reduce the amount of dislocations, resulting in a lower hardness.¹¹ The microhardness of the coatings after annealing is still twice as high as that of annealed bulk copper, which means that dislocation loops are persistent in the annealed samples. The reduction in the microhardness is not homogeneous in all regions of the annealed

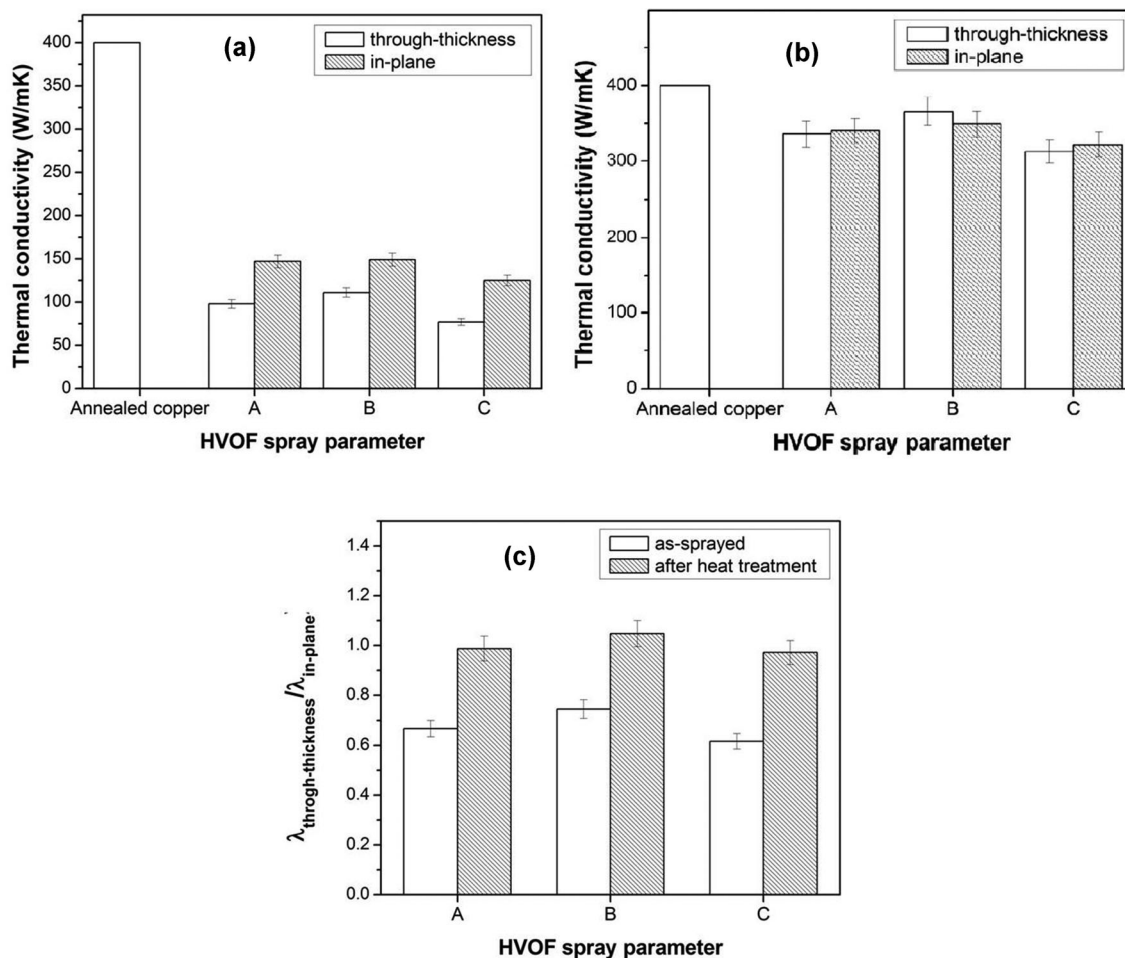


Fig. 2. The through-thickness and in-plane thermal conductivity of (a) as-sprayed and (b) annealed copper coatings. (c) Anisotropy of the thermal conductivity. The value for annealed copper was taken from Ref. 8.

coatings. This effect can be attributed to the differences in the dislocation density across the coating due to the lamellar structure of the HVOF coatings. Areas with lower dislocation density or areas which were already dynamically recrystallized during the coating process require higher recrystallization temperatures than areas with high dislocation density.⁶

Thermal Conductivity

The physical and mechanical properties of thermal spray coatings strongly depend not only on the porosity and oxide content but also on the microstructural features and the nature of the splat interfaces.^{13–17} The through-thickness and in-plane thermal conductivity of the copper coatings are shown in Fig. 2a. The measured thermal conductivity of the coatings was slightly lower than the reported value by Liu et al.⁷ for Cu-coatings on a diamond-Cu substrate. The in-plane thermal conductivity is higher than the through-thickness thermal conductivity in all cases. The oxide content of coatings is two times higher than that of the

initial powder feedstock which is in the range of 0.35–0.37%. Oxide content is affected by the ratio of fuel to oxygen during deposition. By increasing the fuel/oxygen ratio, the oxide content remained almost constant in the coatings. The average length of splats in the two directions shows the number of splat/splat interfaces in each direction (Table SII, supplemental). The number of splats and splat/splat interfaces was decreased by increasing the length of splats in each direction. By decreasing the number of splats, the barriers for electron conduction or phonon dispersion was decreased and the thermal conductivity was increased. The average length of splats in the in-plane direction was longer than that in the through-thickness direction which indicates that the number of splats and barriers were fewer in the in-plane direction. This could explain the lower thermal conductivity measured in the through-thickness direction for all three coatings. Figure 2b shows the thermal conductivity of coatings in both directions after heat treatment for 6 h at 600°C. The thermal conductivity of the annealed coatings was three times higher than those of the as-sprayed

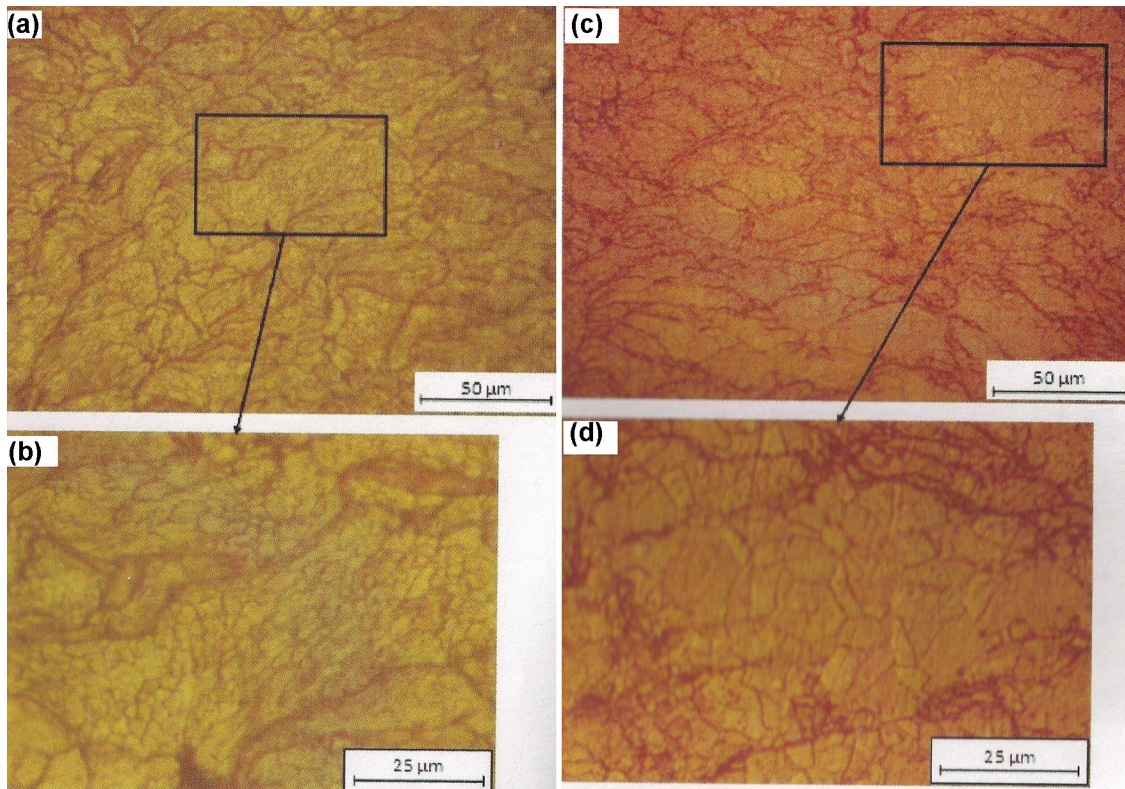


Fig. 3. Optical images from the cross-section of the as-deposited (a, b) and annealed (c, d) copper coatings deposited under spray condition B.

coatings. After annealing, the thermal conductivity of the coatings was close to the thermal conductivity of the annealed copper (400 W/mK). The difference between the thermal conductivity in the two perpendicular directions was reduced after heat treatment. The average length of splats increased after annealing, indicating that the number of barriers decreased after annealing (Table SII, supplemental). Figure 3 shows optical images from the cross-section of the coating deposited under condition B before and after annealing. Higher magnification images from the as-sprayed and annealed microstructures clearly exhibit some splat boundaries elimination and grain growth inside the splats. For the coating deposited under condition B, the average length of the splats was higher than that for the coatings deposited under conditions A and C. Therefore, in both the as-coated and heat treated samples, the spraying condition which generated the lowest number of barriers was spray condition B which produced the coatings with the highest thermal conductivity.

Figure 3c shows the related thermal conductivity anisotropy of the coatings obtained under different spraying conditions. The values closer to 1 show the more isotropic structure of the coating. The values of the anisotropy of the heat-treated coatings are close to 1, which indicates that these structures became more uniform and isotropic after the annealing.

Electrical Resistivity

The average in-plane and through-thickness resistivity of the as-sprayed and heat treated coatings are shown in Fig. 4a and b, and the corresponding anisotropy is plotted in Fig. 4c. The electrical behavior of the coatings is similar to its thermal conductivity. Coatings deposited under spraying condition B exhibited the lowest electrical resistivity. The longest splat length was measured in coatings deposited under condition B (Table SII, supplementary). McCune et al.¹⁸ measured the resistivity of the cold-sprayed copper coating about $2.4 \mu\Omega$. Li et al.⁸ measured the electrical resistivity in two parallel and perpendicular directions for cold-sprayed copper coatings around $2.3 \mu\Omega$ cm and $3.8 \mu\Omega$ cm. They reported that, after annealing at 650°C , the electrical resistivity reduced to $1.7 \mu\Omega$ cm in both directions. The lowest resistivity measured in this study was about $5.2 \mu\Omega$ cm which was obtained in coatings sprayed under condition B. Figure 4c shows that the electrical resistivity of all coatings was reduced after post-deposition heat treatment and in-plane resistivity was still lower than through-thickness resistivity. After heat treatment, the splat length increased (Table SII, supplemental) and the number of splat/splat interfaces decreased, which are the barriers for conduction of electrons across metallic coatings. The resistivity of coatings ($1.9 \mu\Omega$ cm) became close to resistivity of the IACS (International Annealed

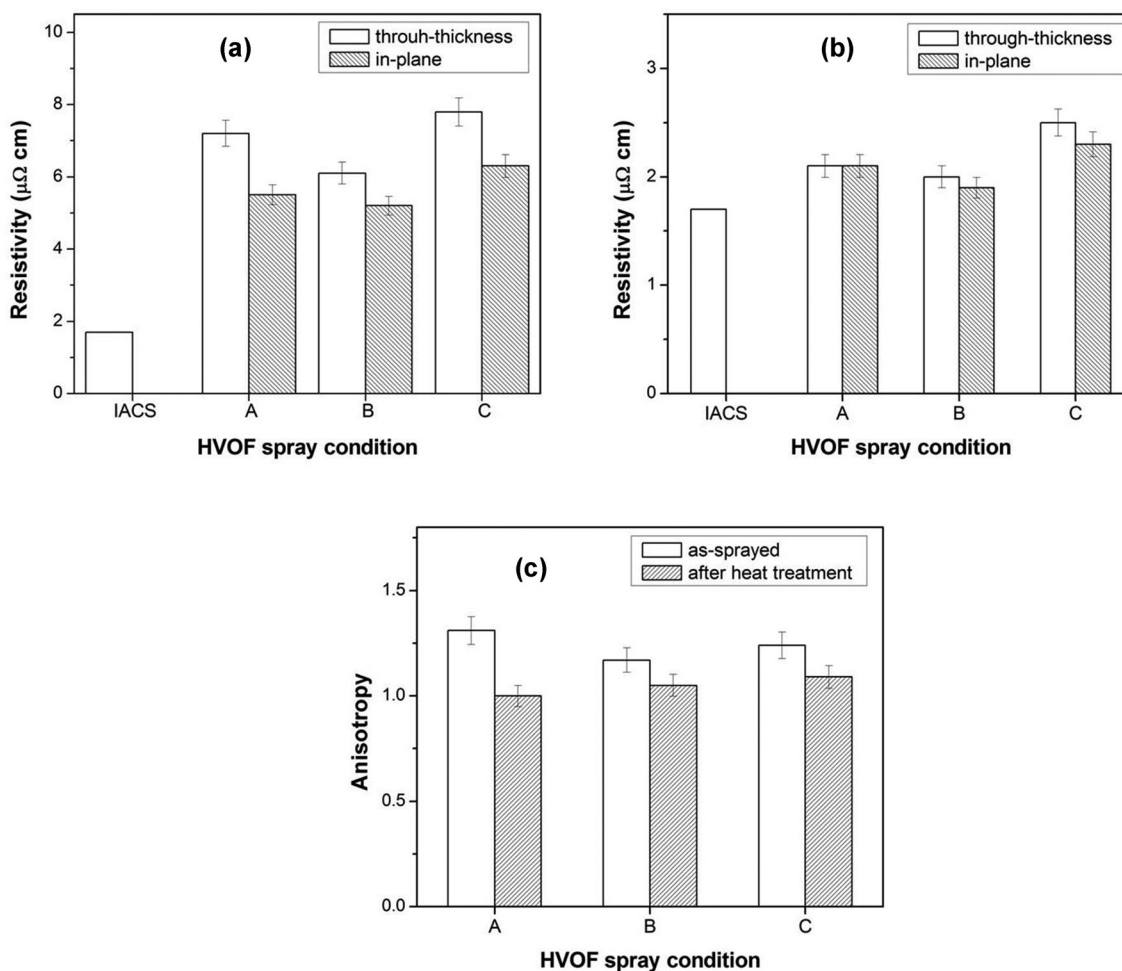


Fig. 4. The through-thickness and in-plane electrical resistivity of (a) as-sprayed and (b) annealed copper coatings. (c) Anisotropy of the electrical resistivity. Value for IACS was taken from Ref. 7.

Copper Standards, 1.7 $\mu\Omega$ cm) after heat treatment.⁸ Also, the resistivity in the through-thickness direction and the in-plane direction were closer to each other and the coatings became more isotropic after heat treatment, as was previously described by the analysis of the thermal conductivity data. Therefore, the annealing treatment can significantly improve the properties of HVOF-sprayed copper coating accompanying the homogenized microstructure.

CONCLUSION

Electrical and thermal characterization of copper coatings deposited by HVOF was carried out with the aim of studying the relationship between the electrical and thermal conductivities and the direction of spraying. As-sprayed copper coatings exhibited different thermal and electrical conductivities in the through-thickness and in-plane directions. These differences were attributed to the average splat length measured in each direction. Other parameters such as oxide content and porosity affect these properties when compared with reference values.

Thermal treatments increased the thermal conductivity, reduced the electrical resistivity values and produced the homogenization of the microstructure, leading to an isotropic behavior of thermal and electrical properties. The differences in the properties of the three spray conditions can be due to the changes in the fuel/oxygen ratio and thus changes in heat input and flattening of the splats.

ACKNOWLEDGEMENTS

Dr. E. Garcia acknowledges the financial support of Project MAT2009-09600 and the Ramon y Cajal Program of the Ministry Economy and Competitiveness of Spain (MINECO).

ELECTRONIC SUPPLEMENTARY MATERIAL

The online version of this article (doi:10.1007/s11837-017-2537-x) contains supplementary material, which is available to authorized users.

REFERENCES

1. C. Borchers, F. Gärtner, T. Stoltenhoff, H. Kreye, and H. Assadi, *J. Appl. Phys.* 93, 10064 (2003).
2. C.-J. Li and A. Ohmori, *J. Therm. Spray Technol.* 11, 365 (2002).
3. A. Sharma, R.J. Gambino, and S. Sampath, *Acta Mater.* 54, 59 (2006).
4. F. Gärtner, T. Stoltenhoff, J. Voyer, H. Kreye, S. Riekehr, and M. Koçak, *Surf. Coat. Technol.* 200, 6770 (2006).
5. M. Schroeder, *J. Therm. Spray Technol.* 7, 325 (1998).
6. T. Stoltenhoff, C. Borchers, F. Gärtner, and H. Kreye, *Surf. Coat. Technol.* 200, 4947 (2006).
7. M. Liu, K. Yang, C.-M. Deng, C.-G. Deng, and K. Zhao, *J. Therm. Spray Technol.* 25, 1516 (2016).
8. W.-Y. Li, C.-J. Li, and H. Liao, *J. Therm. Spray Technol.* 15, 206 (2006).
9. P. Sudharshan Phani, D. Srinivasa Rao, S.V. Joshi, and G. Sundararajan, *J. Therm. Spray Technol.* 16, 425 (2007).
10. C.J. Li and W.Y. Li, *Surf. Coat. Technol.* 162, 31 (2003).
11. C. Borchers, F. Gärtner, T. Stoltenhoff, and H. Kreye, *Acta Mater.* 53, 2991 (2005).
12. W.Y. Li, C.J. Li, and H.L. Liao, *Appl. Surf. Sci.* 256, 4953 (2010).
13. W.Y. Li, X.P. Guo, M. Yu, H.L. Liao, and C. Coddet, *J. Therm. Spray Technol.* 20, 252 (2011).
14. M. Yu, W.Y. Li, X.P. Guo, and H.L. Liao, *J. Therm. Spray Technol.* 22, 433 (2013).
15. S. Sampath, X.Y. Jiang, J. Matejicek, L. Prchlik, A. Kulkarni, and A. Vaidya, *Mater. Sci. Eng. A* 364, 216 (2004).
16. S. Deshpande, A. Kulkarni, S. Sampath, and H. Herman, *Surf. Coat. Technol.* 187, 6 (2004).
17. Z. Wang, A. Kulkarni, S. Deshpande, T. Nakamura, and H. Herman, *Acta Mater.* 51, 5319 (2003).
18. R.C. McCune, W.T. Donlon, O.O. Popoola, and E.L. Cartwright, *J. Therm. Spray Technol.* 9, 73 (2000).